

# CMS Conference Report

---

23 November 2006

## Track and Vertex Reconstruction in CMS

W. Adam<sup>a)</sup>

*Institute of High Energy Physics, Austrian Academy of Sciences, Vienna, Austria*

Talk given at Vertex06, Perugia, Italy  
on behalf of the CMS Collaboration

### **Abstract**

The CMS experiment relies on a Silicon pixel and micro-strip tracker for the reconstruction of tracks and vertices of charged particles in the harsh environment of proton and heavy-ion collisions at the LHC at CERN. An outline of the basic track and vertex reconstruction algorithms used in CMS is given and their performance is described. Results of more advanced algorithms like the Gaussian Sum Filter for electron reconstruction and robust vertex fitters are shown.

# Track and Vertex Reconstruction in CMS

Wolfgang Adam<sup>a,1</sup>

<sup>a</sup>*Institute of High Energy Physics, Austrian Academy of Sciences, Vienna, Austria*

---

## Abstract

The CMS experiment relies on a Silicon pixel and micro-strip tracker for the reconstruction of tracks and vertices of charged particles in the harsh environment of proton and heavy-ion collisions at the LHC at CERN. An outline of the basic track and vertex reconstruction algorithms used in CMS is given and their performance is described. Results of more advanced algorithms like the Gaussian Sum Filter for electron reconstruction and robust vertex fitters are shown.

*Key words:* LHC; CMS; track reconstruction; vertex reconstruction

---

## 1. Introduction

CMS is one of the two general purpose experiments in construction at the LHC at CERN. The LHC environment constitutes an experimental challenge: p-p collisions at the design luminosity of  $10^{34}\text{cm}^{-2}\text{s}^{-1}$  will produce in the order of 20 superimposed events at a rate of 40 MHz, resulting in thousands of tracks in the acceptance of the tracking system (1).

In order to cope with these conditions, track and vertex reconstruction rely on a system of Silicon pixel and micro-strip sensors, embedded in a solenoidal magnetic field of 4T. The high granularity of the sensors results in a low occupancy even for the extremely high flux of charged particles expected from proton and heavy ion collisions at the LHC. The high single point resolution translates into excellent momentum resolution and precise extrapolation of charged particle trajectories

to the interaction region. This allows, in turn, for reconstruction of primary and secondary vertices and for the identification of the decays of long-lived particles. A good estimate of the track parameters at the outer boundary of the tracker provides the link to the other detector systems, in particular the electromagnetic calorimeter and the muon chambers.

A basic set of track and vertex finding and fitting algorithms has been designed for the reconstruction of minimum ionizing particles created in p-p collisions. Minor modifications allow to use it for other applications, e.g. in the CMS High Level Trigger (2) or in the reconstruction of heavy-ion collisions. Individual components can easily be exchanged with more advanced adaptive algorithms which have been shown to improve performance in dense environments and in the presence of non-Gaussian contributions like the radiative energy loss of electrons.

---

<sup>1</sup> on behalf of the CMS Collaboration

## 2. Detector layout

The CMS Tracker consists of an inner pixel system enclosed in layers of micro-strip detectors. Both subsystems comprise a central cylindrical barrel part and two end-caps. In the beam ( $z$ -) direction the systems extends to  $\pm 2.7\text{m}$  from the interaction point; the outer radius is about  $1.1\text{m}$  (3).

The pixel system consists of three barrel layers at radii of  $4.4$ ,  $7.3$  and  $10.2\text{ cm}$  and two sets of turbine-like endcap layers at distances of  $34.5$  and  $46.5\text{ cm}$  on each side of the interaction point. The pixels have a size of  $100 \times 150\mu\text{m}$ .

The rectangular strip sensors in the barrel are arranged in 10 cylindrical layers starting at a radius of about  $20\text{ cm}$ , the strips being parallel to the beam axis. The inner 4 layers consist of thin sensors ( $d = 320\mu\text{m}$ ), the 6 outer layers of thick sensors ( $d = 500\mu\text{m}$ ). The pitch varies with radius from  $80\mu\text{m}$  at the innermost layer to  $183\mu\text{m}$  at the outermost layer, matching the decrease in the charged particle flux and the less stringent requirements on spatial resolution at the outer boundary of the tracker. The two inner layers of each of the two sub-detectors are equipped with pairs of sensors mounted back-to-back with a stereo angle of  $100\text{ mrad}$ .

In each end-cap trapezoidal strip sensors are arranged in planar disks with the strips pointing to the beam line. A first set of three disks complements the inner part of the barrel. A further set of nine disks extends to the outer radius of the barrel system. On the disks sensors are arranged in up to 7 rings with a radial variation of thickness and pitch similar to the one in the barrel. Rings 1, 2 and 5 are equipped with modules in a stereo configuration.

## 3. Track reconstruction

The reconstruction of charged tracks is done in three stages (4). The first stage provides seeds for further reconstruction, based on pairs of hits which are selected to be compatible with the interaction region and a lower  $p_T$  limit, taking into account

multiple scattering (5). Due to the low occupancy and the unambiguous 2-dimensional position information the pixel layers provide the best seeding. The selection of pixel hits is fast and highly efficient. The application of the same algorithm to the inner strip layers extends the acceptance and can provide seeding in the commissioning phase, before installation of the full pixel system (Fig. 1).

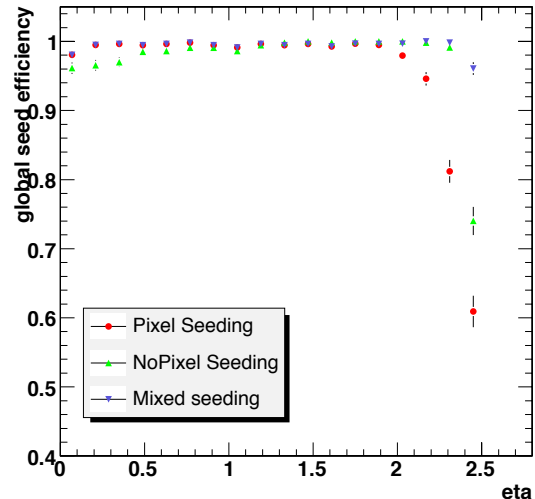


Fig. 1. Hit-pair finding efficiency for muons with  $p_T = 1\text{GeV}/c$  in the pixel detector, in the strip detector and for a combination of both (1).

The second stage uses a first estimate of the track parameters, calculated from the seed, to collect the full set of hits for a charged particle track. It is based on a combinatorial Kalman filter approach: Starting from the current parameters the trajectory is extrapolated to the next layer and compatible hits are selected based on the  $\chi^2$  between the predicted and measured positions. The Kalman update of the predicted parameters with each of these hits provides a new set of trajectory candidates. In order to take into account possible inefficiencies one further candidate is created without including any hit information ("lost" hit). A quality filter is applied to reject poor candidates. The remaining ones are ranked according to their quality and the best ones are retained for further propagation. Ambiguities between tracks sharing a substantial number of hits are resolved during and after track finding. While traversing the tracker the

extrapolation uncertainties in the transverse plane quickly converge on a low level, such that in most cases only one compatible hit is found (Fig. 2). A crucial component of the system is the fast and efficient selection of compatible sensors and hits which is facilitated by the hermeticity of the layers. The pattern recognition can be adapted to the needs of the High Level Trigger system (2).

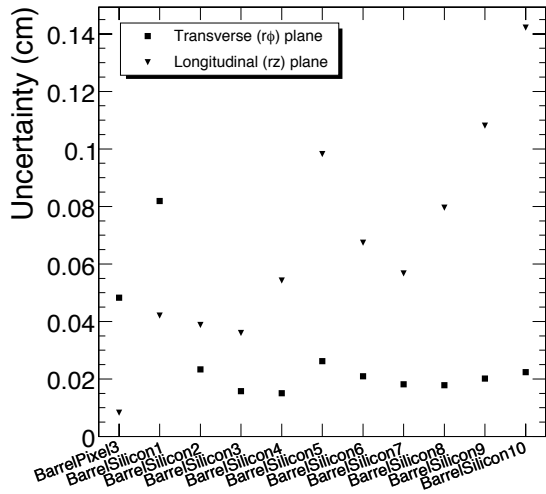


Fig. 2. Average extrapolation uncertainties in the transverse and longitudinal planes during track finding in the barrel part of the tracker as a function of the layer (4).

The third stage consists of a least-squares fit in the form of a Kalman filter for the final estimation of the track parameters. A "forward" fit proceeding outwards from the interaction region removes the approximations used in the track finding stage and provides an optimal estimate of the track parameters at the outside of the tracker. A "backward" fit in the opposite direction yields the estimate of the track parameters in the interaction region and – in combination with the forward fit – at each of the intermediate layers. The momentum resolution is shown in Fig. 3.

The reconstruction is almost fully efficient for muons within the acceptance. The reconstruction of pions suffers from the substantial amount of material present in the tracker. Requiring at least 8 reconstructed hits it varies typically between 80% and 90% depending on momentum and rapidity. At low luminosity ( $2 \times 10^{33} \text{cm}^{-2} \text{s}^{-1}$ ) and using

the same selection the efficiency in b-jets with a  $p_T$  range of 120 - 170 GeV/c is compatible with the one of low momentum pions while the fake rate remains below the percent level.

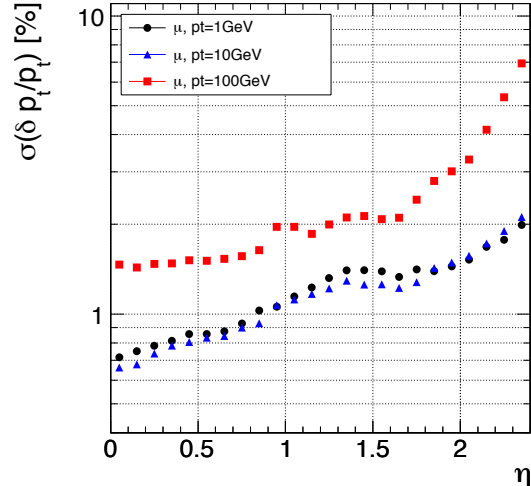


Fig. 3. Normalised momentum resolution for single muons of transverse momenta of 1, 10 and 100 GeV/c (4).

The same algorithms can be tuned to cope with the higher track densities of heavy-ion collisions. Seeding with hit-triplets instead of pairs and avoiding the combination of hits in the stereo layers before tracking keeps the time needed for reconstruction affordable, while tighter quality criteria reduce the fake rate. In simulations of central Pb-Pb-collisions with 3000 - 3500 charged tracks / unit an efficiency at the 80% level could be achieved for fake rates below 10% (6).

Due to their highly non-Gaussian energy loss distribution electrons constitute a special challenge for track reconstruction. Using a "Gaussian Sum Filter" (GSF) (7) this distribution can be modeled and the whole track can be fitted, yielding an estimated probability density function of the track parameters. In Fig. 4 the momentum resolution achieved with the weighted mean of this distribution is compared with the result of a Kalman filter. The reconstructed momenta at the inside and outside of the tracker can be used to estimate the total energy loss in the tracker and to improve the energy measurement of the calorimeter at low momenta (8).

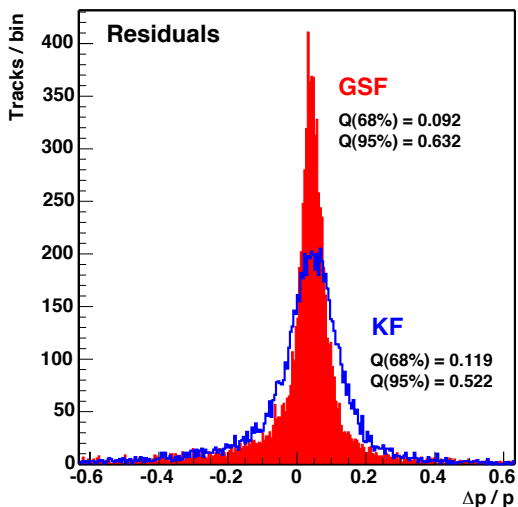


Fig. 4. Normalised momentum residuals for electrons with  $p_T = 10\text{GeV}/c$  in the barrel part of the tracker using the mean value of the momentum distribution estimated by the GSF (filled histogram) and the result of a Kalman filter (open histogram). The numbers correspond to the half-widths of the 68% and 95% coverage intervals (7).

#### 4. Vertex reconstruction

The algorithmic base for vertex finding and fitting is again the Kalman filter (9). Vertex fits have to take into account the possible contamination of the associated tracks with particles from other vertices. The use of robust fit procedures reduces the impact of such outliers on the estimated position. The standard version of a robust fitter is the "trimmed Kalman vertex fitter" (TKF): if the  $\chi^2$ -probability of the least compatible track is  $< 5\%$  the track removed and the fit is re-iterated. An alternative is the "adaptive vertex fitter" (AVF): a weight is assigned to each track as a function of its  $\chi^2$ -contribution. The weights are determined following an annealing procedure in order to avoid local minima. The procedure results in a soft assignment of tracks to vertices, and the number of associated tracks and the  $\chi^2$  of the fit are replaced by an effective number of tracks and a pseudo- $\chi^2$ . The AVF is less sensitive to high levels of contamination. For complex events it has been shown to yield a slightly better vertex position resolution and to be faster than the TKF.

Primary vertex candidates are obtained by

clustering preselected tracks along the beam line, where the preselection is based on the impact parameter significance and  $p_T$ . Vertex candidates are fitted, filtered according to their compatibility with the beam line and their  $\chi^2$  and finally ranked by the sum of the  $p_T^2$  of the associated tracks. The efficiency for reconstructing and correctly tagging the primary vertex of the signal event depends on the number of charged tracks produced at the vertex. For low luminosity it ranges from 76% for  $H \rightarrow \gamma\gamma$  to 99% for  $t\bar{t}H$  events (1).

Secondary vertices are reconstructed with the TKF. After a first fit to the complete set of tracks the ones compatible with the vertex candidate are removed. Further iterations are done with the tracks found to be incompatible with the vertex at previous steps. Secondary vertex candidates are validated using a selection on the distance to the primary vertex and an upper cut on the invariant mass. Decay of b-hadrons result frequently in tertiary vertices. Decay products of these vertices are recovered by selecting tracks close to the flight path between primary and secondary vertex ("tertiary vertex finding"). These tracks are not used to estimate a vertex position but to improve kinematic selections (10). For b-jets in the barrel region and with a  $p_T$  in the range 20 – 70 GeV/c a secondary vertex efficiency of 63% was obtained at a purity of 90%. The track association efficiency of the TKF is 76%. The tertiary vertex finding increases this value by 4% while the purity of the associated tracks is almost unchanged at about 90%. The resolutions for the flight distance for b- and c-vertices are shown in Fig. 5. The results of the secondary vertex reconstruction have been used in a powerful combined b-tagging algorithm (11).

#### 5. Conclusions

The reconstruction of the vertices and trajectories of charged particles is a key element in the analysis of high energy physics data. CMS disposes of a large set of algorithms for an efficient reconstruction of these objects in the high multiplicity environment of the LHC, based on the data of its large Silicon tracker. The standard algorithms for track

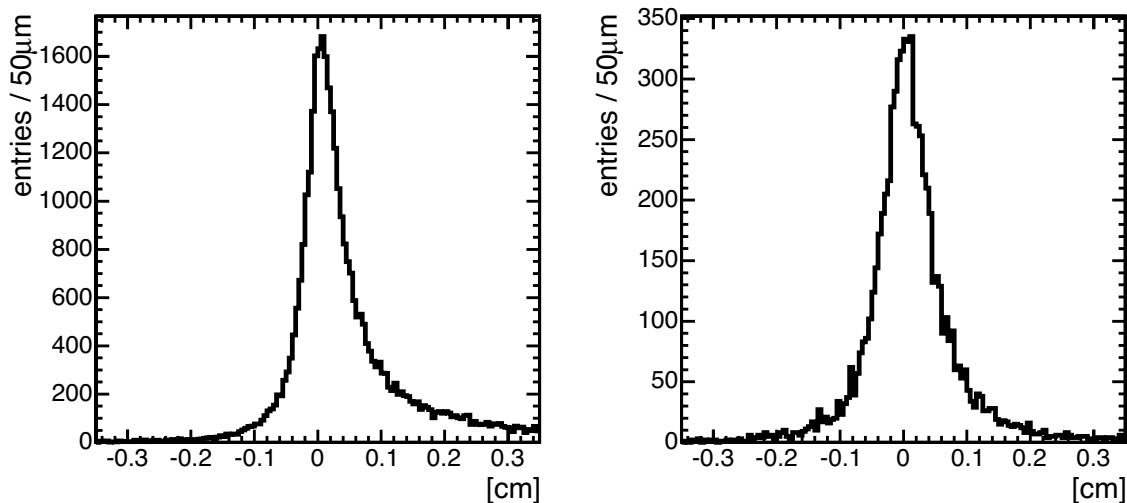


Fig. 5. The resolution on the reconstructed flight distance for b- (left) and c-vertices (right) in the barrel region (10). The 68% coverage is  $765\mu\text{m}$  for b- and  $550\mu\text{m}$  for c-vertices.

and vertex finding and fitting make extensive use of the Kalman filter. They are sufficiently flexible to be adapted for the use in the High Level Trigger and for the reconstruction of heavy ion collisions. A Gaussian sum filter has been implemented for the reconstruction of electron tracks. The robustness of vertex reconstruction has been improved using adaptive fitters.

The performance of track and vertex reconstruction has been demonstrated using simulated events. The CMS Tracker has now entered the phase of integration and commissioning (12). First sets of cosmic ray data recorded in dedicated set-ups, during the integration of sub-detectors and in the CMS "magnet test and cosmic challenge" are available. They have been passed through the reconstruction chain and will help to exercise the calibration and alignment procedures and to test and tune the track reconstruction algorithms.

## References

- [1] CMS Collaboration, *CMS Physics TDR Vol. 1*, **CERN-LHCC/2006-001**.
- [2] M. Vos, *The use of the tracker in the CMS trigger*, these proceedings.
- [3] CMS Collaboration, *The Tracker System Project TDR*, **CERN-LHCC/98-6** and *Addendum to the CMS Tracker TDR*, **CERN-LHCC/2000-016**.
- [4] W. Adam et al., *Track reconstruction in the CMS tracker*, **CMS Note 2006/04**.
- [5] S. Cucciarelli et al., *Track reconstruction, primary vertex finding and seed generation with the Pixel Detector*, **CMS Note 2006/026**.
- [6] C. Roland, *Track Reconstruction in Heavy Ion Events using the CMS Tracker*, **CMS Note 2006/031**.
- [7] W. Adam et al., **J. Phys. G: Nucl. Part. Phys.** **31** (2005) N9-N20.
- [8] S. Baffioni et al., *Electron reconstruction in CMS*, **CMS Note 2006/040**.
- [9] T. Speer et al., *Vertex Fitting in the CMS Tracker*, **CMS Note 2006/032**.
- [10] Th. Müller et al., *Inclusive Secondary Vertex Reconstruction in Jets*, **CMS Note 2006/027**.
- [11] C. Weiser, *A Combined Secondary Vertex Based B-Tagging Algorithm in CMS*, **CMS Note 2006/014**.
- [12] R. D'Alessandro, *CMS Silicon Tracker experience in integration and commissioning*, these proceedings.